

Setting and Coordination Strategy of Over Current Relays in Medium Voltage DNs with DG Integration

Ammar A. MAJEED^{a,1}, Mohamed ABDERRAHIM^a, and Afaneen ALKHAZRAJI^b
*a Department of System Engineering and Automation, University Carlos III of Madrid
Avada de la Universidad 30, 28911, Leganes, Madrid, Spain*
*b Communication Engineering Department, University of Technology-Iraq
Al-Sina'a St, 10066, Baghdad, Iraq*

Abstract. Distributed Generation (DG) embedded with Distribution Networks (DNs) has been developed because its performance has become more efficient and sustainable. This reconfiguration mode increases the short-circuit current (SCC), and subsequently heightens the complexities involved in both the setting and operation of the overcurrent protection system. Therefore, it is necessary to develop a robust protection strategy for DNs integrated with DG to prevent the electrical equipment from collapsing during abnormal conditions. This study proposed one of the most important and reliable strategies for resetting and re-coordinating overcurrent relays (OCRs) that operate in the same protection zone of the distribution feeder. This methodology restricts the main variables and elements used in the protection device (PD) setting after DG is embedded to redesign a suitable setting and coordination. However, international, and national benchmark standards are used to specify suitable equations that satisfy high-protection system characteristics to ensure the reliability of DNs according to a real case study of a medium voltage level 33kV in the electrical distribution feeder of Baghdad, Iraq.

Keywords. over current relay, distribution networks, distributed generation

1. Introduction

The proliferation of DG technologies has experienced notable and substantial growth in recent times, primarily owing to their economic benefits, environmental considerations, and the increase in electricity demand [1]. However, the installation of DG systems in DNs brings about significant changes in their topology and electrical constraints, leading to challenges in protection systems when operating in both grid-connected and islanded configurations. These challenges include increased fault current magnitude, potential obscuration of the protection system, risks of sympathetic or false tripping, and complexities in configuring OCRs [2], [3].

To overcome these challenges and establish a robust, dependable, and secure protection system, it is indispensable to uphold the setting and coordination of the OCRs

¹ Corresponding Author: Ammar A. MAJEED, Department of System Engineering and Automation, University Carlos III of Madrid, Avada de la Universidad 30, 28911, Leganes, Madrid, Spain; Email: ammarabbasmajeed.al-rubaye@alumnos.uc3m.es, ORCID ID <https://orcid.org/0000-0002-6884-9356>

in compliance with the prescribed operating time (OT), both in pre-and post-DG integration while adhering to a standardized time dial setting (TDS) and coordination time interval (CTI). Guaranteeing that the operating hours of OCRs are maximized to attain efficient protection and coordination, the creation of an objective function is essential.

Furthermore, the practical use of simulation techniques to assess the performance of OCRs in a typical electric DN case study significantly improves the ability of planning and design engineers to select the best OCR arrangement and coordination. This choice is based on the voltage level of the DN and the optimized allocation of integrated DG resources.

Initially, the DNs of Baghdad in Iraq were set up in a radial structure. However, the utility had to implement DG to meet the rising load needs because of a shortage in generation capacity. The government also plans to incorporate different type from large and medium-sized DG. Therefore, the contribution of this work is to investigate how these DG units can be integrated into the protection system, particularly concerning OCRs operating in medium voltage DNs that work with scheduled electrical power extinguishing .

This paper is carefully organized, commencing with a comprehensive literature review to provide a foundational context for the investigation's subject matter. Subsequently, an extensive critique of our methodology is presented, encompassing mathematical models, analytical methods, and electrical module design. The outcomes of an in-depth case study or simulation are subsequently presented and scrutinized. The final section contains a summary of the major conclusions and suggestions for future projects.

2. Literature Review

Incorporating DG into a DN necessitates a reevaluation of conventional protection configurations to address challenges, including the adjustment of parameter settings. Minimize the relay operating time and prevent mal-operation in grid-connected and islanded DG interfaced distribution systems by optimizing the TDS suggested in [4]. To enhance coordination within each group, an adaptive approach is introduced. This method uses the available setting groups (SG) and the classification index (CI) to classify different states inside limited setting groups [5]. Moreover, the determination of directional OCR parameters involves assessing downstream and upstream relays in the context of various combinations of singular or multiple DG connections within a radial test system [6]. Upon fault detection, the power from the DG reverses owing to low resistance at the fault point. Consequently, directional overcurrent relays (DOCRs) are employed for DG protection [7]. This relay configuration comprises of overcurrent and directional elements. Coordination relies on relay operation and time-current characteristic curves [8]. Furthermore, even with adequate relay coordination, system stability can be compromised without including a critical clearing time (CCT) as a constraint [9].

Introducing a novel protection philosophy to enhance assertiveness and reliability through the utilization of existing protection device functions. This approach enhances the reliability of the protection system and the assertiveness of any fault [10]. In the event of a fault, impedance calculations inform the relay characteristic to establish the (OT. The relay characteristic is augmented by a function directly linked to the cumulative

impedance observed by the relay [11]. The whale optimization algorithm (WOA) was employed to derive optimal values for the pickup currents (I_{pu}) and TDS of the DOCRs [12]. A comparative analysis was conducted to identify the most efficient method. Various optimization methodologies, including genetic algorithms, artificial bee colonies, harmonic search approaches, firefly techniques, cuckoo search methods, and particle swarm optimization, have been evaluated for their effectiveness in relay coordination. [13]. The authors in [14] proposed a novel OCR protection strategy utilizing digital twins in a DN with DG. These findings indicate a lack of coordination in the existing OCR protection schemes for various DGs. Moreover, a grouping scheme was introduced for setting an interconnected DG through OCRs. A vector is created for each potential ss interconnection within the system and used to classify them into four distinct groups by employing k-means clustering [15]. A novel overcurrent protection function (OCPF) scheme based on IEC 61850, presented in [16], incorporated a directional element. This enhanced scheme augments the existing capabilities to effectively address multiple fault scenarios and accommodate the seamless integration of DG. Importantly, they can be readily deployed within digital substations, eliminating the need for additional equipment installation.

3. Methodology

Overcurrent protection relays are crucial for protecting electrical equipment and human safety during electrical faults or short circuits by detecting and interrupting excessive currents. Notably, the separation of faulty parts is executed by the circuit breaker (CB) operation mechanism, triggered by an overcurrent protection relay (OCR). Ensuring proper coordination among multiple OCRs operating within an electrical system, that may be located at different points but must respond to the same fault is essential. This coordination process can be intricate and requires meticulous evaluation of the DNs.

3.1. Electrical Model and Configuration

The alteration from a radial setup to a bidirectional model due to increased DG integration near the load is visually depicted in Figure 1. which delineates the function

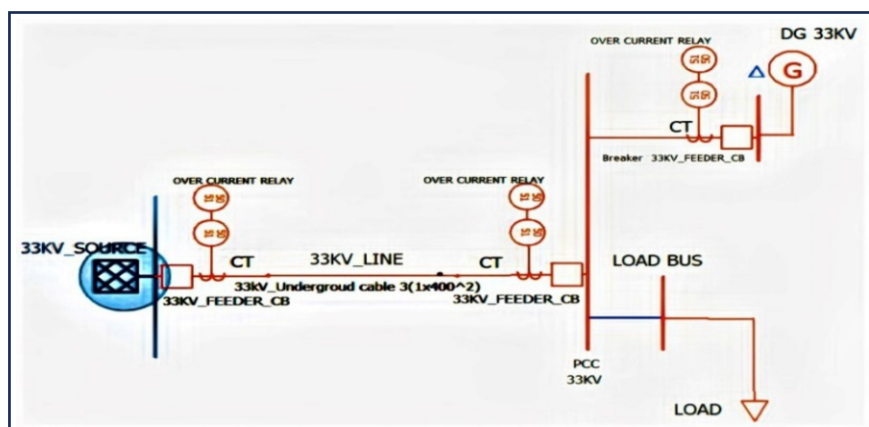


Figure 1. Protection system in 33kV electrical DN model with DG connected near the load.

of the 33kV feeder originating from the source and transferring electrical power to the substation load through the medium voltage of the 33kV distribution line.

The protection of this line against sudden load surges or faults is imperative. Hence, the DNs deploy the OCRs at the feeder start and termination point of the distribution line. This method ensures that the CB functions as both primary and backup protection, opposing the power disturbances arising from the load current. Moreover, it protects the electrical equipment against abnormal currents in both directions, especially in the context of DG integration. Consequently, the OCR within this setup (50/51) responds in alignment with the converted current derived from the 600/5 current transformer (CT). Concurrently, the point of common coupling (PCC) designates the bus bar connection between the utility network and DG. It is essential to isolate this point during periods of light load to separate the DG from the DN in the event of a load current exceeding the I_{pu} or during faults occurring. Subsequently, manual isolation of FEEDER_CB or activation through an OCR signal is implemented.

3.2. Mathematical Formulation and Analytical Approaches

Relays employing inverse time settings are typically categorized as inverse, very inverse, or extremely inverse, each demonstrating different operating speeds within the DN through their characteristic curves. Definite-time OCRs offer evident benefits, particularly in cases of high fault currents, leading to reduced trip durations and ensuring protection selectivity without compromising safety. Accordingly, a combined protection system, utilizing the attributes of inverse definite minimum time (IDMT) along with instantaneous relay settings, is exemplified in Figure 2. [17]. The OCRs can be set up in one of two ways, delay time (DT) and I_{pu} . The maximum load current and minimum fault current must fall within the range of I_{pu} (1) [18].

$$I_{max} \leq I_{pu} \leq I_{min} \quad (1)$$

where I_{max} represents the maximum load current and I_{min} is the minimum SCC.

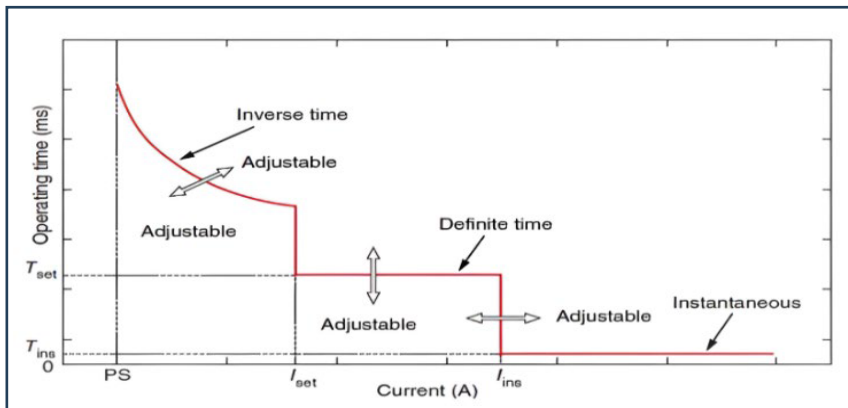


Figure 2. Time-current characteristic curve of Combined OC.

The immediate aspect of relay settings incorporates adjusting the maximum rated current of the DN to approximately five times the full load current when operating in the grid-connected mode. This adjustment considers conditions such as equipment quality, lifespan, and involves using 50% of the maximum short-circuit current I_{sc} as in (2), at

the point where the current transformer supplies inputs for instantaneous relay operation [19].

$$\text{Instantaneous protection unit setting} = 0.5I_{sc} / CTR \quad (2)$$

However, with the progress in software development, it is now easier to select commonly used characteristics by utilizing various algorithms stored in the memory of the microprocessor.

The relay pick-up setting, representing the threshold current and potential fault currents, ranges from 50% to 500% for OCRs with intelligent electronic device (IED) traits. This range is termed the plug-setting multiplier (PSM) or plug setting, indicating the ratio between the secondary CT fault current and the relay's pick-up as in (3). Equation (4) outlines the pick-up setting for phase relays, providing a safety margin beyond the nominal current during overload conditions [20]

$$PSM = \frac{I_f}{I_{pu}} \quad (3)$$

$$\text{plug setting (PS)} = I_{pu} / CTR \quad (4)$$

$$I_{pu} = OLF \times I_{nom} \quad (5)$$

where CTR signifies the current transformer ratio.

The overload factor (OLF) varies depending on the protected equipment and is subject to ranges set by the manufacturer's recommendations, specific application requirements, and the OCR performance category. During emergencies, it is recommended to maintain the load on feeders within DN's at a level that is approximately twice the normal capacity. Typically, the relay's rating pertains to the 100% current setting. $I_{nom} = I_{load}$ represents the maximum normal load current observed by the relay. Under typical operational conditions, the pick-up setting for the earth-fault criteria was chosen while considering the most significant disturbance that could exist within the system.

$$\text{plug setting (PS)} = (0.1 - 0.8) \times I_{nom} / CTR \quad (6)$$

In fault scenarios, the DG current results in elevated fault current levels, as described in Equation (7). This situation may necessitate the incorporation of supplementary Protective Devices (PDs) or modification of existing protection settings and coordination [21].

$$I_{fault} = I_{Grid} + I_{GDG} \quad (7)$$

TDS is a numerical parameter altering the relay's operating time can vary within a range of 0.05 to 1.0 seconds, although many numerical relays permit values as low as 0.025. The boundaries are delineated as [22].

$$TDS_{max} \leq TDS \leq TDS_{min} \quad (8)$$

Here, TDS_{max} and TDS_{min} represent the maximum and minimum TDS values, respectively, as specified by the international standard of the OCR manufacturer.

3.3. Relay Coordination Techniques

Adjusting the PD settings to ensure efficient coordination and reduce the likelihood of false trips or equipment impairment may fall under the category of coordination [23]. The mathematical definition of the operating time is outlined according to the standards established by the IEC, and the IEEE is referenced in the subsequent discussion.

$$T = \frac{TDS \times A}{\left(\frac{I_f}{I_{pu}}\right)^{B-1}} + C \quad (9)$$

In this context:

T : operating time of relay in seconds.

I_{pu} : chosen pickup current.

I_f : denotes the fault current level measured in amperes.

TDS : time dial setting or time multiplier setting.

C stands as a constant within the equation.

The parameters that played a decisive role in establishing the slope of the relay characteristics were A and B . These constants, along with 'C' adhere to the distinct standards for OCRs specified under the IEC and IEEE. Table 1 presents the characteristic attributes for both the classifications. Equation (10) is employed to calculate a reasonable minimum grading time interval, denoted as the GTI , between the two coordinate OCRs.

$$GTI = \left[\frac{2E_R + E_{CT}}{100} \right] t_1 + t_{CB} + t_o + t_s \quad (10)$$

Where:

$2E_R$: relay timing error

E_{CT} : allowance for CT ratio error (%)

t_{CB} : CB interrupts time in seconds. CONSTANTS FOR STANDARD OCRs BASED ON IEC AND IEEE STANDARDS.

t_1 : downstream relay time of operation.

t_o : relay overshoot time in seconds.

t_s : safety margin in seconds.

Table 1. Constants for Standards OCRs based on IEC Standards.

Curve Categories	A	B
Standard (Moderately) Inverse	0.14 (0.0515)	0.02
Very Inverse	13.5 (19.61)	1 (2)
Extremely Inverse	80 (28.2)	2
Long Time Inverse	120	1

The subsequent steps delineate the process of calculating TDS to achieve effective coordination and protection for relays with IDMT characteristics.

- Involves employing the minimum TDS determined by the fault level to ascertain the desired t_1 of the remote relay, which originates from an electric power source.
- Determine t_1 of the relay for the adjacent substation breaker, as indicated in Equation (9). Assume an average downstream time (t_{CB}) of 100 milliseconds (5 cycles), which varies based on elements such as the type, equipment current rating, fault current level, and operating mechanism. Typically, interrupting time falls within the range of 3 to 8 cycles or 60 to 160 milliseconds for a 50Hz system, depending on the application and system requirements. Additionally, consider $E_R=5\%$, $E_{CT}=10\%$, $t_o=20$ milliseconds, and $t_s=30$ milliseconds for digital and numerical OCR [24], [25].

$$td = 0.2t_1 + 0.15 \quad (11)$$

where: relay error factor = $0.2t_1$. td , denoted as the discrimination margin time (DMT) or CTI for a breaker-breaker scenario, is the combined result of t_{CB} , t_o , and t_s , measured in seconds. As per IEEE-242, this interval is commonly approximated in research to fall within the range of 0.2 to 0.5 seconds [26].

$$t_{2a} = t_1 + t_d \quad (12)$$

$$t_d \leq t_{2a} - t_1 \quad (13)$$

where: t_{2a} the operating time desired for the backup relay.

- c) Calculate the TDS for the backup relay using the same fault current as in the previous steps (a and b) and determine t_{2a} at the specified pickup level.

$$TDS_{new} = \frac{\text{Desired operating time } (t_{2a})}{\text{Operating time at selected PSM and TDS 1.0}} \quad (14)$$

- d) Determine the effective time of operation (t_{2b}) for the backup relay, incorporating the fault level and pickup value relevant to its connection point.

$$t_{2b} = OT \text{ under PSM and TDS 1.0} \times TDS_{new} \quad (15)$$

- e) Proceed with the sequence, commencing from step b.

4. Real Case Study Simulation and Finding Discussion

This study focuses on the electrical DN in Baghdad-Iraq. The protection system evaluation of these networks is essential, particularly concerning the penetration of DG to address the demand requirements during power generation shortages. All electrical data were collected from the SCADA system of the Baghdad electricity distribution company at the Iraqi Ministry of Electricity (MOE).

4.1. Description of DN

In Figure 3, a photograph map was generated through the Bagdad-Rusafa municipality and the geographic information system GIS department in the Bagdad-Rusafa electrical distribution directory. To illustrate the 33kV medium voltage feeder. This network facilitated the transfer of power from the 132/33kV New_ADAMIYA substation to the 33/11kV power transformer (TR) number 2 at the AFFAQ substation (2×31.5MVA). The feeder comprised a three-phase underground copper conductor cable with a size of $1 \times 400 \text{ mm}^2$ for each phase conductor and 2 km in length.

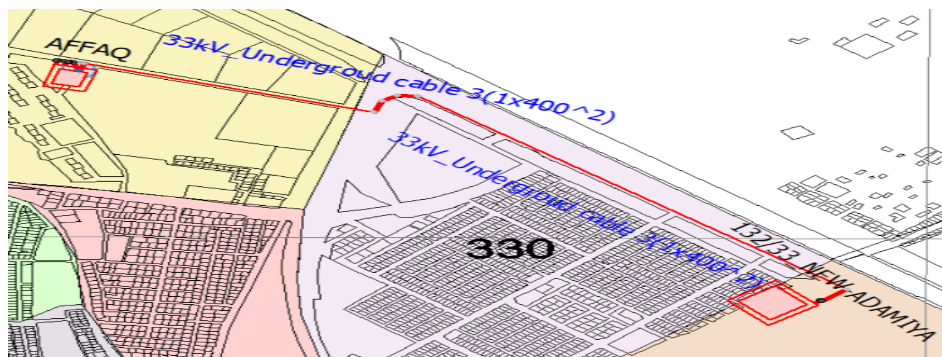


Figure 3. Medium voltage 33kV feeder sources NEW_ADAMIYA 132/33KV to 33/11kV TR.2 in AFFAQ substation.

As per the model depicted in Figure 1. The optimal placement of the DG involves connecting it to the PCC at the AFFAQ substation. Consequently, the protection system undergoes modification post-DG penetration, introducing a new CB with its associated OCRs. These elements require precise configuration and coordination with the existing

protective devices (PDs) in both the protection zones of the source and load terminals. Furthermore, two main features of OCRs operate in radial distribution feeders depending on the fault's current types, phase, and ground fault properties. In this real case, the OCR types that operates on the source side is (SIEMENS 7SJ600) and on the load terminal side in the AFFAQ substation is (ALSTOM MICOM). This study depended on a load power factor (pf) of 0.9 in line with the worst measured value in this real network.

4.2. Simulation Result and Discussion

- Before DG integration with DN

In addition to the I_{pu} of 600 Ampere, which is calculated according to the maximum load current of (437.8) Ampere multiplied by the *OLF* of (1.37). The SCC must be calculated to determine the boundaries of the OCR setting. The CYMEDist 9.0 r4 program was used to obtain the results shown in Table 2. explain the detailed operational timings and additional factors of the phase OCR according to the phase faults (LLL, LLG, LL) and some main additional fault points. According to the MOE specifications, the medium voltage equipment should be designed to withstand an SCC of 25kA for 1 second.

Table 2. Factors and Operating Time of Phase OCR-IDMT with Instantaneous for all Fault Types in AFFAQ_C.B.

	TDS = 0.1 as in MOE			$I_{pu} = 600A$			C.T. ratio = 600/5			PS = 5	
Fault types	Minimum fault Ampere			Maximum fault Ampere			Additional point Ampere				
	LLL	LLG	LL	LLL	LLG	LL	1.1 Ipu	41.67 Ipu			
	3900	3404	3377	8586	7668	7436	660	25000			
OT in Sec.	0.376	0.397	0.398	0.256	0.268	0.271	9.501	0.227			
Instantaneous:				$I_{pu} = 3000 A$			DT = 0.050 sec.				

Moreover, with little difference in the load current measured the source CB of (436.7 Ampere) because of losses in cable resistance. The same analysis simulated the results shown in Table 3.

Table 3. Factors and Operating Time of Phase OCR-IDMT with Instantaneous for All Fault Types in NEW_ADAMIYA_C.B.

	TDS = 0.2			$I_{pu} = 600A$			C.T. ratio = 600/5			PS = 5	
Fault types	Minimum fault Ampere			Maximum fault Ampere			Additional point Ampere				
	LLL	LLG	LL	LLL	LLG	LL	1.1 Ipu	41.67 Ipu			
	8586	7668	7436	9306	8296	8059	660	25000			
OT in Sec.	0.512	0.536	0.542	0.479	0.471	0.473	14.68	0.453			
Instantaneous:				$I_{pu} = 3600 A$			DT = 0.210 sec.				

Conversely, analogous procedures are employed for ground fault analysis to determine the optimal configuration and coordination for both source and load OCRs. Table 4, and Table 5. elucidate the factors and results of operating times for various ground faults (LLG, LG), emphasizing the key fault locations.

Table 4. Factors and operating time of ground OCR-IDMT with instantaneous for all fault types in AFFAQ_C.B.

	TDS = 0.1 as in MOE			$I_{pu} = 60A$			C.T. ratio = 600/5			PS = 0.5	
	Minimum fault Ampere			Maximum fault Ampere			Additional point Ampere				

Fault types	LLG	LG	LLG	LG	2 Ipu	10 Ipu
	3403.6	105.2	7668	924.2	120	600
OT in Sec.	0.050	1.244	0.050	0.294	1.006	0.297
Instantaneous:			$I_{pu} = 180 \text{ A}$	DT = 0.050 sec.		

Table 5. Factors and operating time of ground OCR-IDMT with instantaneous for all fault types in NEW_ADAMIYA_C.B.

	TDS = 0.2		$I_{pu} = 60 \text{ A}$		C.T. ratio = 600/5		PS = 0.5	
Fault types	Minimum fault Ampere		Maximum fault Ampere		Additional point Ampere			
	LLG	LG	LLG	LG	2 Ipu	10 Ipu		
	7668	924.2	8295.5	944	120	600		
OT in Sec.	0.050	0.498	0.050	0.494	2.010	0.594		
Instantaneous:			$I_{pu} = 210 \text{ A}$	DT = 0.21 sec.				

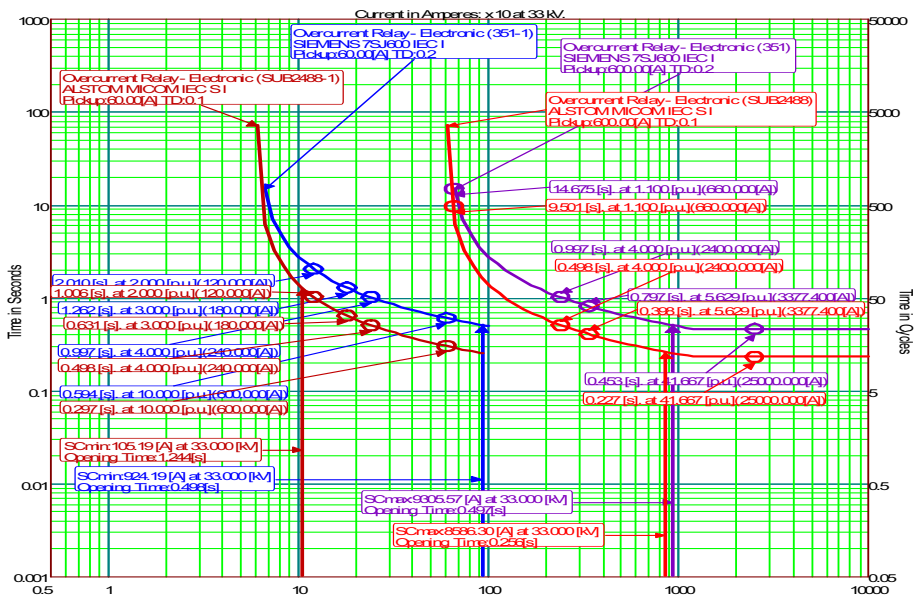


Figure 4. The TCCC for the phase and ground OCR-IDMT on both side of the 33 kV feeder.

Figure 4. illustrates the Time-Current Characteristics Curve (TCCC) for both the phase and ground OCRs within the circuit breakers protecting the 33kV feeder on the right and left sides of the figure respectively, and for both the source and load sides.

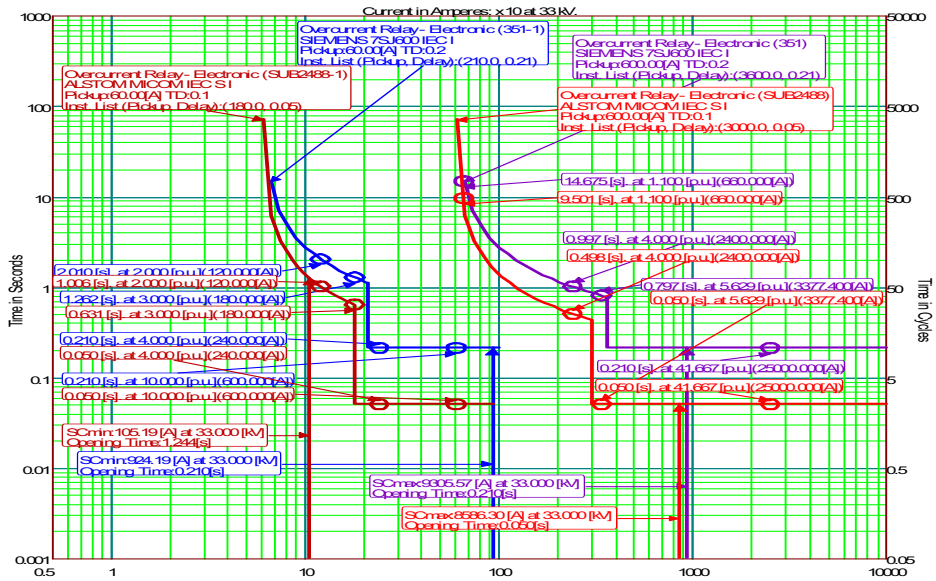


Figure 5. The TCCC for the phase and ground OCR-IDMT on both side of the 33 kV feeder with instantaneous.

Meanwhile, Figure 5. describes the TCCC incorporating the instantaneous feature. The OCRs based on the formulated model and key aspects guarantee secure operation and heightened reliability in protecting the equipment against load current and SCC.

- After DG integration with DN

The medium-voltage DN encompasses diverse forms of DG, and for this specific case, study DG with an estimated *pf* of 0.9 is considered suitable. This choice is informed by the proximity of the available space near the substation, as shown in Figure 3. Furthermore, the selection of the AFFAQ substation for DG integration is not arbitrary; it is grounded in the optimal allocation findings from previous research [27]. Accordingly, this section aims to design an optimal setting and coordination, considering the evolving requirements resulting from the integration of DG. The load current is anticipated to decrease from the utility source to 155.4 Amperes, with the DG supplying the residual load current at 274.7 Amperes. Consequently, the *OLF* settings for both the main and backup OCRs were adjusted to 1.9 and 1.28, respectively. In contrast, the OCR setting for the DG station was set at 1.06. Table 6. explains the factors of the new phase-OCR added to the network as PD for the DG station and the operation time against different phase fault types.

Table 6. Factors and operating time of phase OCR-IDMT with instantaneous for all fault types in DG_C.B.

	TDS = 0.1 as in MOE $I_{pu} = 290A$			C.T. ratio = 300/5 PS = 4.85	
Fault types	Phase faults Ampere			Additional point Ampere	
		LLL	LLG	LL	1.138 I _{pu}
	8526	7498	7265	330	25000
OT in Sec.	0.227	0.227	0.227	5.576	0.227
Instantaneous:			$I_{pu} = 1450 A$	DT = 0.050 sec.	

Table 7, and Table 8 delineate the revised setting and coordination design, encompassing all the relevant parameters for the phase OCRs at both the AFFAQ and NEW_ADAMIYA substations. These tables elucidate the alterations in the operating time attributable to heightened SCC following the integration of DG. Coordination efforts aim to maintain the CTI at an appropriate level, necessitating corresponding updates to the instantaneous features in response to this variation.

Table 7. Factors and operating time of phase OCR-IDMT with instantaneous for all fault types in AFFAQ_C.B after DG integration.

		TDS = 0.2			$I_{pu} = 300A$			C.T. ratio = 600/5		PS = 2.5	
Fault types	Minimum fault Ampere			Maximum fault Ampere			Additional point Ampere				
	LLL	LLG	LL	LLL	LLG	LL	1.1 Ipu	83.31 Ipu			
	8526	7498	7265	8858	7787	7552	330	25000			
OT in Sec.	0.453	0.453	0.453	0.453	0.453	0.453	19.002	0.453			
Instantaneous:				$I_{pu} = 1500 A$			DT = 0.210 sec.				

Table 8. Factors and operating time of phase OCR-IDMT with instantaneous for all fault types in NEW_ADAMIYA_C.B after DG integration.

		TDS = 0.3			$I_{pu} = 300A$			C.T. ratio = 600/5		PS = 2.5	
Fault types	Minimum fault Ampere			Maximum fault Ampere			Additional point Ampere				
	LLL	LLG	LL	LLL	LLG	LL	1.1 Ipu	83.31 Ipu			
	8586	7787	7552	9578	8416	8175	330	25000			
OT in Sec.	0.680	0.680	0.680	0.680	0.680	0.680	22.012	0.680			
Instantaneous:				$I_{pu} = 1800 A$			DT = 0.410 sec.				

Additionally, the Ipu, TDS, and PS elements were adjusted as secondary settings for OCRs in the DG grid-connected mode. Additionally, the instantaneous current decreases because of the lower load currents in comparison to the scenario without DG. The delay time was modified to align with the benchmark and meet the specified requirements of the MOE. For the ground fault types, Table 9, Table 10, and Table 11 describe the factors of ground OCRs to DG, AFFAQ_CB, and NEW_ADAMIYA_CB respectively.

Table 9. Factors and operating time of ground OCR-IDMT with instantaneous for all fault types in DG_C.B

		TDS = 0.1 as in MOE		$I_{pu} = 30A$		C.T. ratio = 300/5		PS = 0.5			
Fault types	Phase faults Ampere		Additional point Ampere								
	LLG	LG	2 Ipu	10 Ipu							
	7498.2	915	60	300							
OT in Sec.	0.227	0.227	1.006	0.297							
Instantaneous:				$I_{pu} = 90 A$		DT = 0.050 sec.					

Table 10. Factors and operating time of ground OCR-IDMT with instantaneous for all fault types in AFFAQ_C.B after DG integration.

		TDS = 0.2		$I_{pu} = 30A$		C.T. ratio = 600/5		PS = 2.5			
Fault types	Minimum fault Ampere		Maximum fault Ampere		Additional point Ampere						
	LLG	LG	LLG	LG	2 Ipu	10 Ipu					
	7498.2	915	7787.4	925	60	300					
OT in Sec.	0.453	0.453	0.453	0.453	2.011	0.594					
Instantaneous:				$I_{pu} = 90 A$		DT = 0.210 sec.					

Table 11. Factors and operating time of ground OCR-IDMT with instantaneous for all fault types in NEW_ADAMIYA_C.B after DG integration.

Fault types	TDS = 0.3		$I_{pu} = 30A$		C.T. ratio = 600/5		PS = 0.5	
	Minimum fault Ampere		Maximum fault Ampere		Additional point Ampere			
	LLG	LG	LLG	LG	2 Ipu	10 Ipu		
	7787.4	925	8415	944.2	60	300		
OT in Sec.	0.680	0.680	0.680	0.680	3.015	0.891		
Instantaneous:			$I_{pu} = 105 A$		DT = 0.410 sec.			

Furthermore, the ground feature serves as a secondary protective measure against the phase feature in the OCR during LLG faults. The setting components underwent adjustments corresponding to variations in fault levels. The CT ratio remains unchanged, as in the scenario without DG, due to its association with the fixed range of the CT equipment. Figure 6. describes the TCCC for phase OCRs on the right side and ground on the left side after DG penetration.

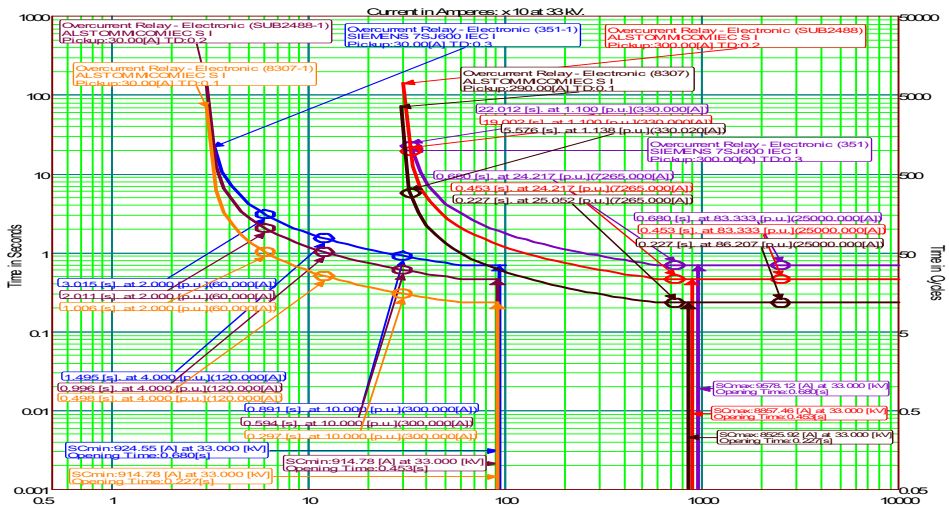


Figure 6. The TCCC for the phase and ground OCR-IDMT on both side of the 33 kV feeder with OCR of DG_CB

It is designed to detect all types of phase or ground faults by OCR in the DG_CB to ensure separate DG stations during disturbances. Subsequently, the original OCRs for the AFFQ_CB near the load and NEW_ADAMIYA from the power source operate as primary and backup protection to separate the faulted feeder. This protection sequence is designed to avoid the DG island operation mode. This depiction provides evidence of the reliability of both the configuration conditions and CTI, ensuring robust protection against a spectrum of conceivable ground fault types and magnitudes. Finally, Figure 7. plots the TCCC for the same OCRs with instantaneous features for the phase and ground fault types.

It is important to avoid the miscoordination between the primary and backup OCRs in addition to ensuring the setting criteria satisfy the resilience of the protection system with and without DG penetration. Although specific operational time outcomes surpass

one second, it is crucial to recognize that this aligns with anticipated standards. These standards adhere to the design aspects of electrical equipment, engineered to withstand fault currents of up to 25kA for one second, following the IEC standards that underpin MOE specifications.

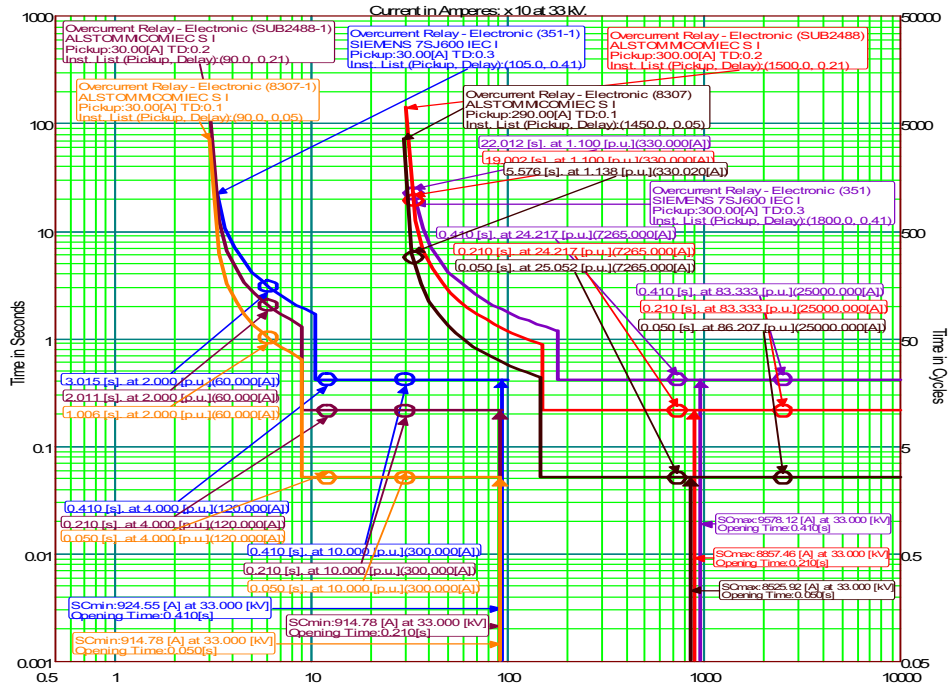


Figure 7. The TCCC for the phase and ground OCR-IDMT on both side of the 33 kV feeder with instantaneous and OCR of DG_CB

5. Conclusions

This study addresses the operational challenges of OCRs in DN with DG integration. The introduction of 15MW DG at the PCC near TR 2 in the AFFAQ 33/11kV substation resulted in an increased SCC, impacting the OCR setting and coordination. Consequently, a recalibration of the primary protection components revealed an elevation in TDS from 0.1 to 0.2, subsequently influencing the backup set to 0.3. These adjustments were implemented across various points to detect both phase and ground faults for the two OCR parameter settings before and after DG integration. Utilizing the CYMDist program, a dedicated tool for electrical DN analysis, facilitated the determination of SCC, load current, and plotting of TCCC using IDMT relays. Additionally, the fluctuation in the load current necessitated the precise calculation of the I_{pu} , an important factor in the OCR setting.

The research also delved into maintaining the CTI within benchmark boundaries, aligning with the OCR manufacturing characteristics designed for this real-case study. As a prospective avenue, the proposed strategy can be extended to 11kV and low voltage DN, incorporating green distributed generation within environmentally sensitive areas.

Acknowledgement

The gratitude to the Iraqi MOE for the provision of data.

References

- [1] A. Farshadi, B. K. Eydi, H. Nafisi, H. Askarian-Abyaneh, and A. Beiranvand, "Rate of Change of Direct-Axis Current Component Protection Scheme for Inverter-Based Islanded Microgrids," *IEEE Access*, vol. 11, no. April, pp. 46926–46937, 2023, doi: 10.1109/ACCESS.2023.3272502.
- [2] H. C. Seo, "Protection Scheme Based on Fault Area Estimation in Loop-Type Low Voltage DC Distribution System with Photovoltaic System using Derivative of Current and Power at Tie Switch," *J. Electr. Eng. Technol.*, vol. 18, no. 4, pp. 3321–3334, 2023, doi: 10.1007/s42835-023-01377-3.
- [3] M. Bindi, M. C. Piccirilli, A. Luchetta, and F. Grasso, "A Comprehensive Review of Fault Diagnosis and Prognosis," *energies, MDPI*, vol. 16, no. 21, pp. 1–37, 2023, doi: 10.3390/en16217317.
- [4] N. K. Choudhary, S. R. Mohanty, and R. Kumar Singh, "Coordination of Overcurrent Relay in Distributed System for Different Network Configuration," *J. Power Energy Eng.*, vol. 03, no. 10, pp. 1–9, 2015, doi: 10.4236/jpee.2015.310001.
- [5] R. Mohammadi, M. Farokhifar, H. A. Abyaneh, and E. Khoob, "Optimal coordination of overcurrent relays in the presence of distributed generation using an adaptive method," *J. Electr. Eng. Technol.*, vol. 11, no. 6, pp. 1590–1599, 2016, doi: 10.5370/JEET.2016.11.6.1590.
- [6] S. C. Ilik and A. B. Arsoy, "Effects of Distributed Generation on Overcurrent Relay Coordination and an Adaptive Protection Scheme," in *IOP Conference Series: Earth and Environmental Science*, 2017, vol. 73, no. 1, p. 012026. doi: 10.1088/1755-1315/73/1/012026.
- [7] T. Kosaleswara Reddy, T. Devaraju, M. Vijaya Kumar, and Y. Paparayudu, "Coordination of over current relays in distributed generation," *Int. J. Recent Technol. Eng.*, vol. 8, no. 2, pp. 5836–5840, 2019, doi: 10.35940/ijrte.B3765.078219.
- [8] J. S. Farkhani, M. Zarecin, H. Soroushmehr, and H. M. Siecee, "Coordination of Directional Overcurrent Protection Relay for Distribution Network With Embedded DG," in *2019 5th Conference on Knowledge Based Engineering and Innovation (KBEI)*, 2019, pp. 281–286.
- [9] S. Khan, "Coordination of Over-Current Relays in Power Distribution Networks with DG Coordination of Over-Current Relays in Power Distribution Networks with DG Considering Transient Stability Constraint," in *Proceedings of IOE Graduate Conference, 2019-Winter*, 2020, no. December 2019, pp. 79–83.
- [10] S. P. S. Matos, M. C. Vargas, L. G. V. Fracalossi, L. F. Encarnaç o, and O. E. Batista, "Protection philosophy for distribution grids with high penetration of distributed generation☆," *Electr. Power Syst. Res.*, vol. 196, no. March, p. 107203, 2021, doi: 10.1016/j.epsr.2021.107203.
- [11] N. H. Torshizi, H. Najafi, and A. S. Noghabi, "Improving Coordination and Operating Speed of Overcurrent Relay against Contingency of Presence of Distributed Generators," *Tabriz J. Electr. Eng.*, vol. 51, no. 1, pp. 33–47, 2021.
- [12] A. Y. Hatata, A. S. Ebeid, and M. M. El-Saadawi, "Optimal restoration of directional overcurrent protection coordination for meshed distribution system integrated with DGs based on FCLs and adaptive relays," *Electr. Power Syst. Res.*, vol. 205, no. October 2021, p. 107738, 2022, doi: 10.1016/j.epsr.2021.107738.
- [13] T. M. Vala, V. N. Rajput, and A. S. Al-Sumaiti, "Investigating the performance of non-standard characteristics-based overcurrent relays and their optimum coordination in distributed generators connected networks," *IET Gener. Transm. Distrib.*, vol. 17, no. 13, pp. 2978–2995, 2023, doi: 10.1049/gtd2.12851.
- [14] E. G mez-Luna, J. E. Candelo-Becerra, and J. C. Vasquez, "A New Digital Twins-Based Overcurrent Protection Distribution Networks," *energies, MDPI*, vol. 16, no. 14, 2023.

- [15] M. N. Alam, S. Chakrabarti, and A. K. Pradhan, "Protection of Networked Microgrids Using Relays with Multiple Setting Groups," *IEEE Trans. Ind. Informatics*, vol. 18, no. 6, pp. 3713–3723, 2022, doi: 10.1109/TII.2021.3120151.
- [16] T. Penthong, M. Ginocchi, A. Ahmadifar, F. Ponci, and A. Monti, "IEC 61850-Based Protection Scheme for Multiple Feeder Faults and Hardware-in-the-Loop Platform for Interoperability Testing," *IEEE Access*, vol. 11, no. March, pp. 65181–65196, 2023, doi: 10.1109/ACCESS.2023.3280128.
- [17] Ali R. Al-Roomi, *Optimal Coordination of Power Protective Devices with Illustrative Examples*, First. Hoboken, New Jersey: John Wiley & Sons, Inc., 2022.
- [18] S. Chowdhury, S. P. Chowdhury, and P. Crossley, *Microgrids and active distribution networks*. 2009. doi: 10.1049/pbrn006e.
- [19] R. Relays, "Application Book Ct Requirements for Ge Multilin," 2016.
- [20] A. Adrianti, E. Asharry, and M. Nasir, "A Distribution Line Protection Scheme for Network with Distributed Generation," *J. Nas. Tek. Elektro*, vol. 10, no. 2, 2021, doi: 10.25077/jnte.v10n2.920.2021.
- [21] F. C. Sampaio, F. L. Tofoli, L. S. Melo, G. C. Barroso, R. F. Sampaio, and R. P. S. Leão, "Adaptive fuzzy directional bat algorithm for the optimal coordination of protection systems based on directional overcurrent relays," *Electr. Power Syst. Res.*, vol. 211, no. June, pp. 1–13, 2022, doi: 10.1016/j.epsr.2022.108619.
- [22] T. E. Sati and M. A. Azzouz, "Optimal Protection Coordination for Inverter Dominated Islanded Microgrids Considering N-1 Contingency," *IEEE Trans. Power Deliv.*, vol. 37, no. 3, pp. 2256–2267, 2022, doi: 10.1109/TPWRD.2021.3108760.
- [23] E. K. Sangkar, F. Namdari, and M. Doostizadeh, "Reconfiguring Distribution Networks by Minimizing Power Loss and Considering Overcurrent Protection," *Int. J. Ind. Electron. Control Optim.*, vol. 4, no. 3, pp. 321–331, 2021.
- [24] Velimir Lackovic, "Overcurrent Protection Fundamentals," *Continuing Education and Development, Inc.*, no. 877. 2017.
- [25] ALSTOM, "Network Protection & Automation Guide," *Alstom Grid Alstom Grid Worldwide Contact Centre*. Alstom Grid Alstom Grid Worldwide Contact Centre www.alstom.com/grid/contactcentre, pp. 336–351, 2011.
- [26] F. Alasali et al., "Advanced Coordination Method for Overcurrent Protection Relays Using New Hybrid and Dynamic Tripping Characteristics for Microgrid," *IEEE Access*, vol. 10, pp. 127377–127396, 2022, doi: 10.1109/ACCESS.2022.3226688.
- [27] A. A. Majeed, "Optimal Distributed Generation Allocation and Protection Coordination of a Distribution Network in Iraq. Master Degree of Science in Electric Power Engineering, A Thesis Submitted to University of Technology, Iraq," 2016.